

Study of possible systematics in the $L_X^* - T_a^*$ correlation of Gamma Ray Bursts

Maria Giovanna Dainotti¹, Vincenzo Fabrizio Cardone^{2,3}, Salvatore Capozziello^{3,4}, Michal Ostrowski¹, Richard Willingale⁵

ABSTRACT

Gamma Ray Bursts (GRBs) are the most energetic sources in the universe and among the farthest known astrophysical sources. These features make them appealing candidates as standard candles for cosmological applications so that studying the physical mechanisms for the origin of the emission and correlations among their observable properties is an interesting task. We consider here the *luminosity* L_X^* - *break time* T_a^* (hereafter LT) correlation and investigate whether there are systematics induced by selection effects or redshift dependent calibration. We perform this analysis both for the full sample of 77 GRBs with known redshift and for the subsample of GRBs having canonical X-ray light curves, hereafter called *U0095* sample. We do not find any systematic bias thus confirming the existence of physical GRB subclasses revealed by tight correlations of their afterglow properties. Furthermore, we study the possibility of applying the LT correlation as a redshift estimator both for the full distribution and for the canonical lightcurves. The large uncertainties and the non negligible intrinsic scatter make the results not so encouraging, but there are nevertheless some hints motivating a further analysis with an increased *U0095* sample.

Subject headings: Gamma Rays: Bursts, Radiation Mechanisms: Nonthermal

¹Obserwatorium Astronomiczne, Uniwersytet Jagielloński, ul. Orła 171, 31-501 Kraków, Poland, E-mails: mariagiovannadainotti@yahoo.it, mio@oa.uj.edu.pl

²Dipartimento di Scienze e Tecnologie dell' Ambiente e del Territorio, Università degli Studi del Molise, Contrada Fonte Lappone, 86090- Pesche (IS), Italy, E-mail: winnyenodrac@gmail.com

³Dipartimento di Scienze Fisiche, Università di Napoli "Federico II", Complesso Universitario di Monte Sant'Angelo, Edificio N, via Cinthia, 80126 - Napoli, Italy E-mail: capozziello@na.infn.it

⁴I.N.F.N., Sez. di Napoli, Complesso Universitario di Monte Sant' Angelo, Edificio G, via Cinthia, 80126 - Napoli, Italy

⁵Department of Physics & Astronomy, University of Leicester, Road Leicester LE1 7RH, United Kingdom, E-mail: rw@star.le.ac.uk

1. Introduction

The high fluence values (from 10^{-7} to 10^{-5} erg/cm²) and the huge isotropic energy emitted ($\simeq 10^{50} - 10^{54}$ erg) at the peak in a remarkably short prompt emission phase make GRBs the most violent and energetic astrophysical phenomena. Fifty years after their discovery in the '60s by the Vela satellites, the nature of GRBs is still unclear. Notwithstanding the variety of their peculiarities, some common features may be identified by looking at their light curves. GRBs have been traditionally classified as *short* ($T_{90} < 2s$) and *long* ($T_{90} > 2s$), although some recent studies (see, e.g., Norris & Bonnell 2006) have revealed the existence of an intermediate class (IC) thus asking for a revision of this criterium. Consequently, long GRBs have now been divided into two classes, *normal* and *low luminosity*, the latter one likely being associated with Supernovae. Here, we concentrate our attention on the class of normal long bursts, observed in X-ray with the aim of better clarifying their origin in the view of possible systematics. A valid tool in classifying GRBs is provided by the analysis of their light curves. The data observed by the Beppo-Sax satellite (Piro 2001) were reasonably well fitted by a simple phenomenological power-law expression, $f(t, \nu) \propto t^{-\alpha} \nu^{-\beta}$ with $(\alpha, \beta) \simeq (1.4, 0.9)$. However, a crucial breakthrough in this field has been represented by the launch of the *Swift* satellite in 2004. The *Swift* instrumental setup, composed by the *Burst Alert Telescope* (BAT, 15 – 150 keV), the *X-Ray Telescope* (XRT, 0.3 – 10 keV) and the *Ultra-Violet/Optical Telescope* (UVOT, 170 – 650 nm), allows a rapid follow-up of the afterglows in different wavelengths giving better coverage of the GRB light curve than the previous missions. Such data revealed the existence of a more complex phenomenology with different slopes and break times thus stressing the inadequacy of a single power-law function. A significant step forward has been made by the analysis of the X-ray afterglow curves of the full sample of *Swift* GRBs showing that they may be fitted by a single analytical expression (Willingale et al. 2007) which we referred to in the following as the W07 model.

It is worth stressing that finding out a universal feature would allow us to recognize if GRBs are standard candles looking for correlations among their observables. The $E_{iso} - E_{peak}$ (Amati et al. 2009), $E_{\gamma} - E_{peak}$ (Ghirlanda et al. 2006), $L - E_{peak}$ (Schaefer 2003) and $L - V$ (Riechart et al. 2001) correlations are some of the attempts pursued in this direction. However, the problem of large data scatter in the considered luminosity relations (Butler et al. 2009; Yu et al. 2009) and a possible impact of detector thresholds on cosmological standard candles (Shahmoradi & Nemiroff 2009) have been discussed controversially (Cabrera et al. 2007). Within this wide framework, we consider here the LT correlation between the break time $T_a^* = T_a/(1+z)$ and the luminosity at the break time L_X^* where z is the GRB redshift and with asteriks we refer to the rest frame quantities. Both these observables refer to the plateau phase of the W07 model. Dainotti et al. (2008) first found that these quantities are not independent, but rather follow the log-linear relation,

$\log L_X^* = a \log T_a^* + b$, with a and b fixed by the fitting procedure. The LT correlation has then been confirmed (Ghisellini et al. 2008; Yamazaki 2009) and recently updated with 77 GRBs (Dainotti et al. 2010) leading to the discovery of a new subclass of the afterglows with smooth observed X-ray light curves, which are preferentially distributed at higher luminosities than the full distribution.

The plan of the paper is as follows. In Section 2, we review the LT correlation explaining how the interested quantities are evaluated and the calibration procedure adopted. Selection effects are discussed in Section 3, while the problem of a possible evolution with z of the calibration parameters is addressed in Section 4. Section 5 investigates the possibility of using the LT correlation as a redshift indicator, while a summary of the results is finally given in Section 6.

2. The LT correlation

The LT correlation relates the time scale T_a^* and the X-ray luminosity L_X^* at T_a , where T_a is defined as the end of the plateau phase. Having had the confirmation of the existence of the above correlation (Dainotti et al. 2010), we here try to answer the question: *Is it affected by systematics?*

As a preliminary remark, let us remember how the quantities of interest are evaluated. The source rest frame luminosity in the *Swift* XRT bandpass, $(E_{min}, E_{max}) = (0.3, 10)$ keV, is computed as:

$$L_X^*(E_{min}, E_{max}, t) = 4\pi D_L^2(z) F_X(E_{min}, E_{max}, t) \cdot K \quad (1)$$

where $D_L(z)$ is the GRB luminosity distance at redshift z , F_X is the measured X-ray energy flux (in erg/cm²/s) and K is the K-correction. Denoting with $f(t)$ the *Swift* light curve and following Bloom et al. (2001), we get:

$$KF_X(E_{min}, E_{max}, t) = f(t) \times \frac{\int_{E_{min}/(1+z)}^{E_{max}/(1+z)} E\Phi(E)dE}{\int_{E_{min}}^{E_{max}} E\Phi(E)dE} \quad (2)$$

with $\Phi(E)$ the differential photon spectrum. We model this term as $\Phi(E) \propto E^{-\gamma_a} \propto E^{-(\beta_a+1)}$ where (β_a, γ_a) are the spectral and photon index, respectively. It is worth stressing that the fit of the model $\Phi(E)$ is performed considering only the spectrum of the plateau phase, selected using a filter time fixed as $T_a \pm \sigma_{T_a}$; the T_a values together with their errorbars, σ_{T_a} , are derived in the fitting procedure (Willingale et al. 2007). As shown also in previous XRT

spectral analysis (Nousek et al. 2006), this particular choice of the filter time leads to the single power-law function as a better fit than the more commonly assumed Band function (Band et al. 1993). According to the W07 model, the functional expression for $f(t)$ is:

$$f(t) = f_p(t) + f_a(t) \quad (3)$$

where the first term accounts for the prompt (the index "p") γ -ray emission and the initial X-ray decay, while the second one describes the afterglow (the index "a"). Both components are modeled with the same functional form:

$$f(t) = \begin{cases} F_c \exp\left(\alpha_c - \frac{t\alpha_c}{T_c}\right) \exp\left(-\frac{t_c}{t}\right) & \text{for } t < T_c \\ F_c \left(\frac{t}{T_c}\right)^{-\alpha_c} \exp\left(-\frac{t_c}{t}\right) & \text{for } t \geq T_c \end{cases} \quad (4)$$

where $c = p$ or a . The transition from the exponential to the power law occurs at the point (T_c, F_c) where the two functional sections have the same value and gradient. The parameter α_c is the temporal power law decay index and the time t_c is the the initial rise time scale. We refer to Willingale et al. (2007) for further details on the analysis, while we only remind here that a usual χ^2 fitting of the $\log(\text{flux})$ vs $\log(\text{time})$ data provides estimates and uncertainties on the time parameters $(\log T_p, \log T_a)$ and the products $(\log F_p T_p, \log F_a T_a)$.

For the afterglow part of the light curve, we have computed values L_X^* (eq. 6) at the time T_a , which marks the end of the plateau phase and the beginning of the last power law decay phase. We have considered the following approximation which takes into accounts the functional form, f_a , of the afterglow component only:

$$f(T_a) \approx f_a(T_a) = F_a \exp\left(-\frac{T_p}{T_a}\right) \quad (5)$$

where we set $t_a = T_p$ because in most cases the afterglow component is fixed at the transition time of the prompt emission, T_p . Actually, we are using Eq.(5), instead of (3) since the contribution of the prompt component is typically smaller than 5%, much lower than the statistical uncertainty on $f_a(T_a)$. Neglecting $f_p(T_a)$ thus allows to reduce the error on $F_X(T_a)$ without introducing any bias. This latter error is then estimated by simply propagating those on β_a , $\log T_a$ and $\log F_a T_a$ thus implicitly assuming that their covariance is null. Inserting Eqs.(5) and (2) into Eq.(1), one then obtains:

$$L_X^* = \frac{4\pi D_L^2(z) F_X}{(1+z)^{1-\beta_a}} \quad (6)$$

where $F_X = F_a \exp(-T_p/T_a)$ is the observed flux at the time T_a .

As a final important remark, we note that the presence of the luminosity distance $D_L(z)$ in Eq.(6) constrains us to adopt a cosmological model to compute L_X^* . We then use a flat Λ CDM model so that the luminosity distance reads :

$$D_L(z) = \frac{c}{H_0} (1+z) \int_0^z \frac{dz'}{\sqrt{\Omega_M(1+z')^3 + (1-\Omega_M)}}. \quad (7)$$

In agreement with the WMAP seven year results (Komatsu et al. 2010), we set $(\Omega_M, h) = (0.272, 0.704)$ with h the Hubble constant H_0 in units of 100 km/s/Mpc.

2.1. Calibration parameters

Let us suppose that R and Q are two quantities related by a linear relation

$$R = aQ + b \quad (8)$$

and denote with σ_{int} the intrinsic scatter around this relation. Calibrating such a relation means determining the two coefficients (a, b) and the intrinsic scatter σ_{int} . To this aim, we will resort to a Bayesian motivated technique (D' Agostini 2005) thus maximizing the likelihood function $\mathcal{L}(a, b, \sigma_{int}) = \exp[-L(a, b, \sigma_{int})]$ with :

$$L(a, b, \sigma_{int}) = \frac{1}{2} \sum \ln(\sigma_{int}^2 + \sigma_{R_i}^2 + a^2 \sigma_{Q_i}^2) + \frac{1}{2} \sum \frac{(R_i - aQ_i - b)^2}{\sigma_{int}^2 + \sigma_{R_i}^2 + a^2 \sigma_{Q_i}^2} \quad (9)$$

where the sum is over the \mathcal{N} objects in the sample. Note that, actually, this maximization is performed in the two parameter space (a, σ_{int}) since b may be estimated analytically as :

$$b = \left[\sum \frac{R_i - aQ_i}{\sigma_{int}^2 + \sigma_{R_i}^2 + a^2 \sigma_{Q_i}^2} \right] \left[\sum \frac{1}{\sigma_{int}^2 + \sigma_{R_i}^2 + a^2 \sigma_{Q_i}^2} \right]^{-1} \quad (10)$$

so that we will not consider it anymore as a fit parameter. The above formulae easily applies to our case setting $R = \log L_X^*(T_a)$ and $Q = \log T_a^*$. We estimate the uncertainty on $\log L_X^*(T_a)$ by propagating the errors on $(T_a, T_p, F_a T_a, \beta_a)$.

The Bayesian approach used here also allows us to quantify the uncertainties on the fit parameters. To this aim, for a given parameter p_i , we first compute the marginalized likelihood $\mathcal{L}_i(p_i)$ by integrating over the other parameter. The median value for the parameter p_i is then found by solving:

$$\int_{p_{i,min}}^{p_{i,med}} \mathcal{L}_i(p_i) dp_i = \frac{1}{2} \int_{p_{i,min}}^{p_{i,max}} \mathcal{L}_i(p_i) dp_i . \quad (11)$$

The 68% (95%) confidence range $(p_{i,l}, p_{i,h})$ are then found by solving:

$$\int_{p_{i,l}}^{p_{i,med}} \mathcal{L}_i(p_i) dp_i = \frac{1 - \varepsilon}{2} \int_{p_{i,min}}^{p_{i,max}} \mathcal{L}_i(p_i) dp_i , \quad (12)$$

$$\int_{p_{i,med}}^{p_{i,h}} \mathcal{L}_i(p_i) dp_i = \frac{1 - \varepsilon}{2} \int_{p_{i,min}}^{p_{i,max}} \mathcal{L}_i(p_i) dp_i , \quad (13)$$

with $\varepsilon = 0.68$ (0.95) for the 68% (95%) range respectively.

3. Threshold selection of the fit error parameter

Dainotti et al. (2010, hereafter D10) have recently updated the LT correlation using a sample of 77 GRBs with known redshift and *Swift* X-ray afterglow light curves. D10 have defined a fit error parameter $u \equiv \sqrt{\sigma_{L_X}^2 + \sigma_{T_a}^2}$, measured in the burst rest frame, to analyze how accuracy of fitting the canonical lightcurve, (eq. 3 and 4) to the data influences the studied correlations. This definition is used to distinguish the canonical shaped light curves from the more irregular ones, perturbed by secondary flares and various non uniformities. D10 have then defined a fiducial sample selecting only GRBs with $u < 4$ and excluding the IC objects thus selecting 62 out of the original 77 GRBs. To be consistent with D10, we here still consider only the fiducial sample. As a general remark, we would like to stress that the study of a whatever correlation among GRBs observables should involve only physically homogenous subsamples thus motivating our exclusion of the IC GRBs because of their different properties from the long ones that mainly constitute our sample. In other words, with homogenous sample we indicate a subsample of GRBs that have lightcurves well defined, in the sense that the Willingale model represents with very good accuracy the parameters values representing the afterglow and the plateau. As a consequence this subsample tightly obeys to the correlation and from this evidence we infer that the properties of the GRBs in this subset are the same. For example, the XRFs are included in the subsample, since they

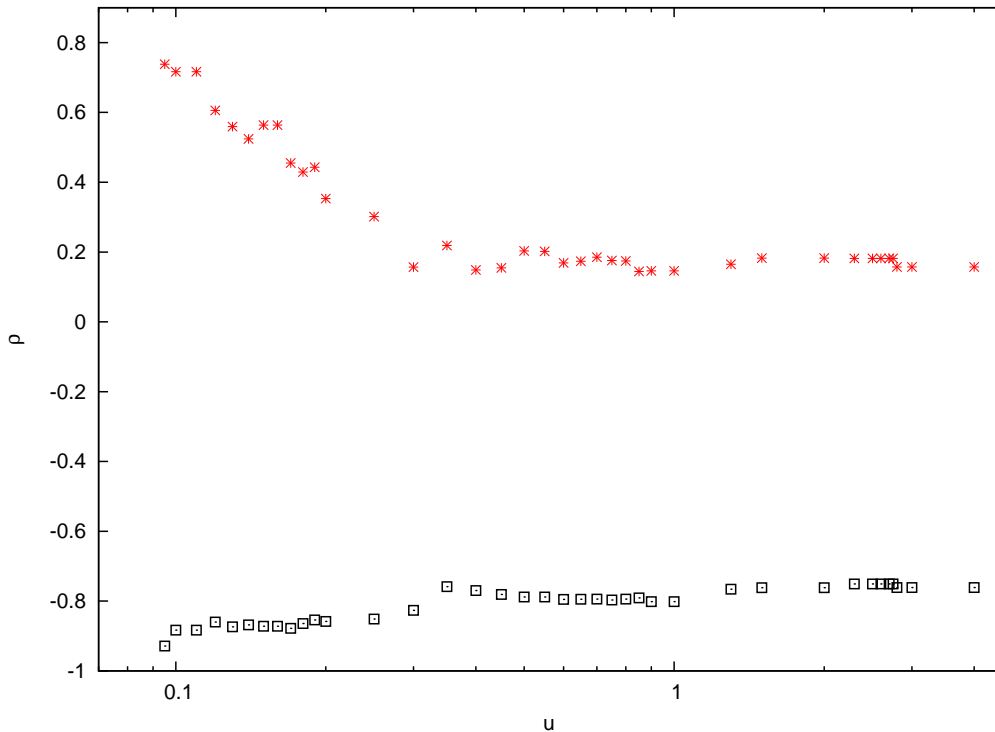


Fig. 1.— Spearman correlation coefficients for the $L_X^* - T_a^*$ (black squares) and $\beta_a - T_a^*$ (red asterisks) as function of the threshold u value.

obey to the correlations, giving in this way evidence to the theory according to which they have the same progenitor mechanism of the normal long GRBs.

As a first indicator for the existence of a relation, we use the Spearman correlation coefficient ρ (Spearman 1904) providing a non-parametric measure of the statistical significance of the dependence between two quantities. Fig. 1 shows $\rho_{LT} = \rho(L_X^*, T_a^*)$ as a function of the threshold u_{th} value, used to exclude from the fiducial sample GRBs with $u > u_{th}$. As we can note, the smaller u_{th} is, the larger ρ is, i.e. the more we are confident that a statistically meaningful correlation indeed exists. The same figure also shows a similar analysis for $\rho_{\beta T} = \rho(\beta_a, T_a^*)$ suggesting that also the slope β_a of the GRB spectrum and the break time T_a^* are correlated. It is worth noting that the smaller u , the smaller the error on $(\log T_a^*, \log L_X^*)$ is. Examining the light curves, we find that small errors are obtained for the GRBs that follow better the W07 model. We therefore argue that both the LT and $\beta_a - T_a^*$ correlations are statistically meaningful provided the GRBs in the sample belong to the class well described by the W07 model.

In order to better investigate the impact of the u selection, we fit the LT correlation to

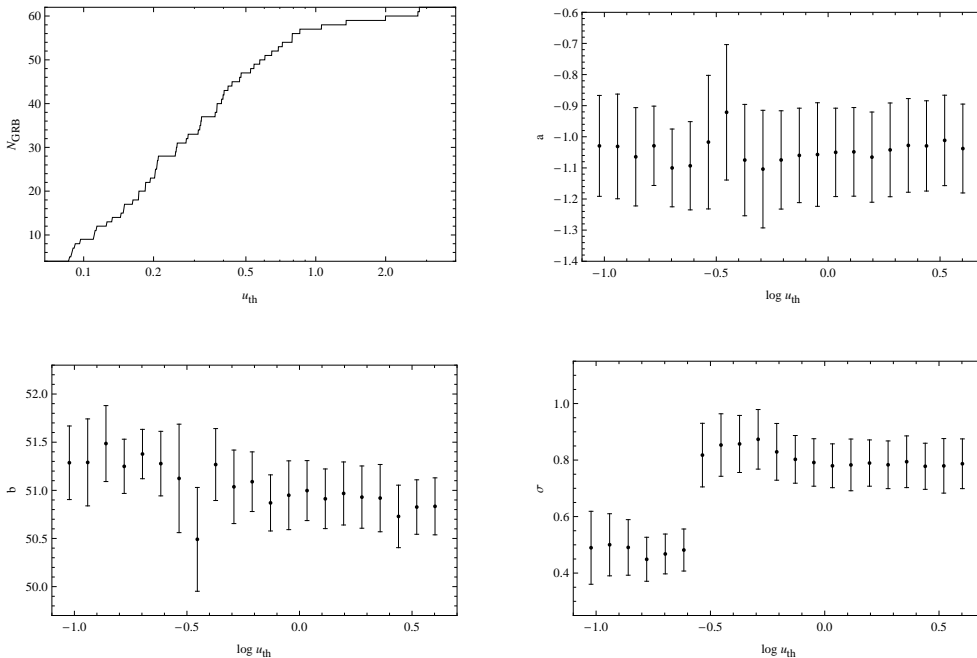


Fig. 2.— Number of GRBs, calibration parameters (a , b) and intrinsic scatter σ_{int} as function of the threshold u_{th} value. See text for a detailed discussion.

GRBs subsamples obtained by selecting only those objects with $u < u_{th}$ with u_{th} running from 0.095 to 4 in steps of 0.01 (with $u_{th} = 4$ for the fiducial sample and $u_{th} = 0.095$ for the canonical ones). The upper left panel in Fig. 2 shows that the number of GRBs in the sample obviously increases with u_{th} , but the price to pay is including GRBs with large errors on $(\log T_a^*, \log L_X^*)$. Such large uncertainties may be due to bad sampling or to a less precise determination of the parameters fitted within the W07 model. In both cases, the estimated values of the fit parameters ($\log T_p, \log T_a, \log F_a T_a$) are not reliable so that it is a safer option to not include large u GRBs in the analysis of correlations. Our chosen value $u = 4$ represents a compromise between the need to assemble a statistically meaningful sample and avoiding uncertain couples $(\log T_a^*, \log L_X^*)$ that can unnecessarily increase the intrinsic scatter.

As a first interesting result, we find that the intrinsic scatter σ_{int} is smaller for smaller u_{th} selected samples, with a sharp drop for $u_{th} = 0.4$. The high values of ρ_{LT} and the decreasing scatter point towards a scenario where the GRBs most deviating from the LT correlation are actually the ones with the less precise determination of the fitted parameters consistent with our guess that their estimated values of $\log T_a^*$ and $\log L_X^*$ are not reliable.

It is worth wondering whether selecting on u biases the calibration parameters (a , b).

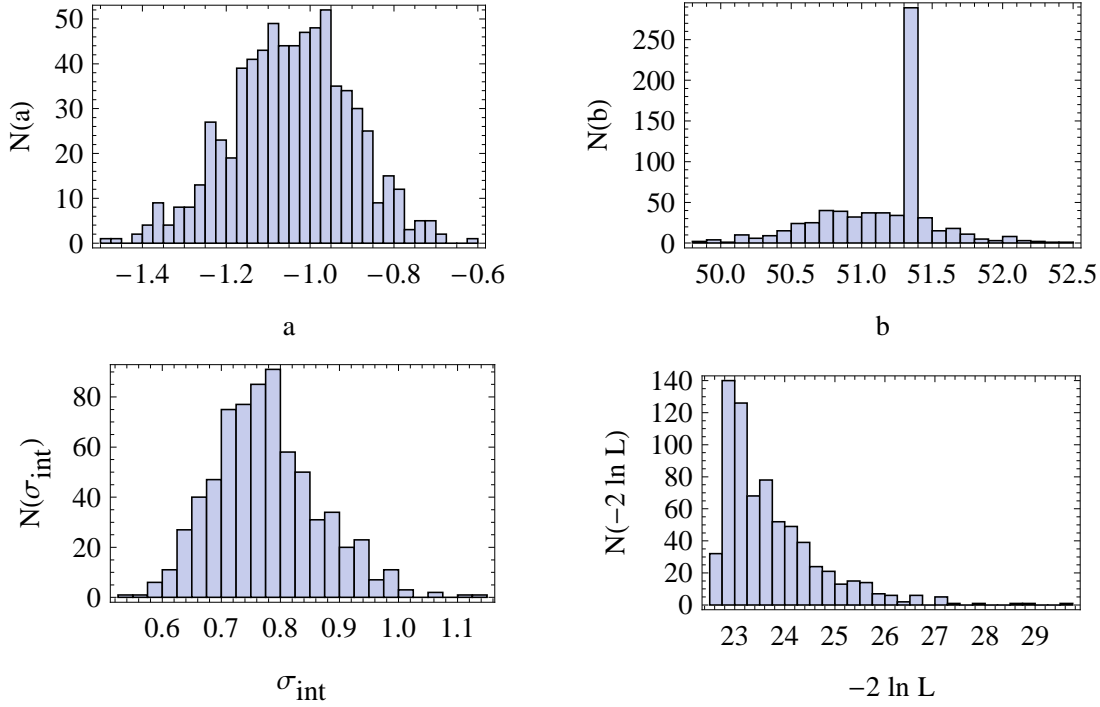


Fig. 3.— Distributions of (a, b, σ_{int}) and $-\ln L$, defined by Eq.(9), for the fiducial sample (62 GRBs with $u < 4$).

Upper right and lower left panels in Fig.2 indeed shows a clear increase of b as u_{th} gets smaller, while the slope a of the correlation remains almost constant at the value $a \simeq -1.06$, consistent with the results in D10 that the small u GRBs (referred to as canonical GRBs in D10) define an subsample $U0095$ for the LT correlation. Actually, one has also to consider the error bars on the fitted parameters although we remember that b is actually correlated to a and σ_{int} being analitically set by Eq.(10). When the large error bars are taken into account, a can indeed be considered independent on u_{th} , while the trend with u_{th} of the zeropoint b remains meaningful. We place here a general explanation on the size of the error bars presented in Fig. 2, Fig. 5, Fig. 7 and Fig. 8, namely how the uncertainties on the calibration parameters have been derived. The size of the uncertainties does not reflect only the scatter in the data in the plots, in fact we can note that they are greater than 1σ , since they reflect also the intrinsic scatter in the law $\log L_X^* = a \log T_a^* + b$. Furthermore, in Fig. 5 the errorbars represented are not directly obtained from the Equ. 6 but they are computed as the median absolute deviation from the median of the parameters. The median values of the observables in the GRBs lightcurves present highly scatter since they reflect intrinsic inhomogeneities in the parameters values. As discussed in detail in our previous papers (Dainotti et al. 2008; Dainotti et al. 2010), the constraints on (a, b, σ_{int}) have been obtained

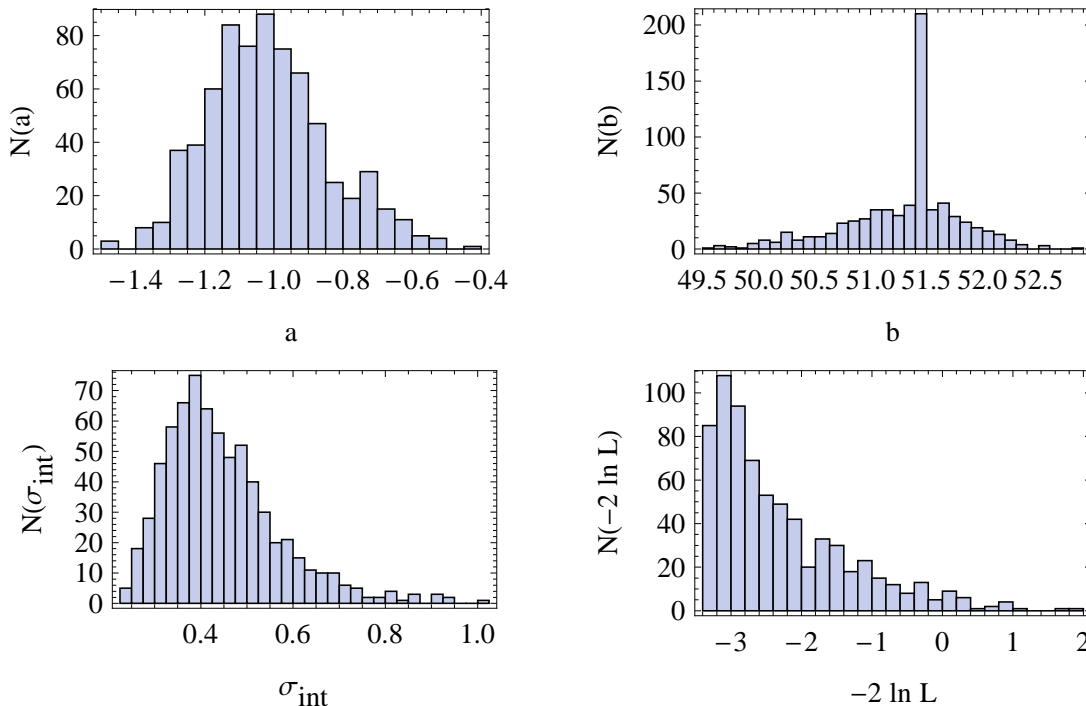


Fig. 4.— Same as Fig. 3 but for the UP sample (8 GRBs with $u < 0.095$).

by running a Monte Carlo Markov Chain algorithm to explore the parameter space (a, σ_{int}) , while b is analytically derived through Eq.(10). To this end, we run two chains, check convergence through the Gellman-Rubin test (Gelman & Rubin 1992) and finally merge them to estimate the median value and the 68% and 95% confidence ranges. Figs.3 and 4 show these histograms ¹ for the fits to the 77 GRBs with $u < 4$ and the U0095 sample. Therefore, the error bars in Fig.2 are determined not only by the scatter in the data, but also by the degeneracies among the model parameters. Moreover, being the distributions mildly asymmetric, the 68% confidence range should not be meant as 1σ error although we use these abuse of terminology for sake of simplicity. When comparing the results of

¹A caveat is related to the high peak in the b histogram. Because of parameters degeneracy, there will be different possibilities to get a value of b close to the best fit one. Since the code preferentially selects models with (a, σ_{int}) as close as possible to the best fit parameters, we will get a lot of couples (a, σ_{int}) giving almost the same b value. In order to show the full b distribution, we have chosen a range much larger than what is actually needed so that the central bin (i.e., the one which the best fit b lies within) will be much more populated than the other ones hence explaining the peak in the figures. Note also that the first bin in the $P(-2 \ln L)$ plots is less populated because it is the one corresponding to the best fit parameters. In order to reach convergence, the MCMC code must first find the best fit and then move away from here so that the first bin is not the most populated one.

the fits to the different u selected samples, one should therefore compare the histograms on (a, b, σ_{int}) and then consider the calibration parameters of different fits in agreement if the corresponding histograms well overlap. This is, for instance, the case for the fiducial and U0095 samples. We note that the median values of the distributions are different, being $(a, b, \sigma_{int}) = (-1.04, 51.30, 0.76)$ for the fiducial sample and $(a, b, \sigma_{int}) = (-1.05, 51.40, 0.40)$ for the U0095 one. However, the histograms for a well overlap so that we find no statistical meaningful difference, while this is the case for both b (although weak) and σ_{int} . The error bars plotted in Fig. 2 allow a quick check for the samples with varying u making us confident that the trends commented above based only on the median values are statistically meaningful.

Up to now, we have interpreted the selection on u as a way to find out the GRBs most closely following the W07 model. It is worth wondering whether such a selection biases in some way the sample by selecting only, e.g., high luminosity GRBs or the shortest ones. To this end, we show in Fig. 5 the median values (with the median deviation) of $(\log L_X^*, \log T_a^*, \beta_a)$ as function of the threshold value used for the error parameter u . As these plots clearly show, there is no trend of the median values of $(\log L_X^*, \log T_a^*, \beta_a)$ with u , namely the invariance of u with respect to $(\log L_X^*, \log T_a^*)$ corresponds directly to invariance in the samples that result when GRBs are chosen for certain u . Indeed, even neglecting the large error bars ², the median values keep constant showing that the samples selected by imposing $u \leq u_{th}$ sample the same region in the parameter space $(\log L_X^*, \log T_a^*, \beta_a)$. This is due to the fact that the definition of u depends directly on $\sigma_{L_X^*}^2$ and $\sigma_{T_a^*}^2$. Therefore, the direct dependence on the possible biases on the sample depends on the parameter values that characterize u . Nevertheless, to be confident that correlation among the parameters will not affect the sample selection we have tested also the median values of β_a vs u , because there is an indication of a correlation among $\log T_a$ vs β_a especially for the limiting $u = 0.095$ sample, (Dainotti et al. 2010). All the tests described clearly shows that the selection on u is only a way to find out the GRBs following as close as possible the Willingale’s model, but this criterion don’t bias the samples. As a consequence, we can conclude that the smaller scatter of the LT correlation for canonical GRBs is not a product of selection effects, but rather the outcome of a (still to be understood) physical mechanism.

A careful inspection of the $\log L_X^*$ vs $\log T_a^*$ plot suggests that the most deviating points are the low luminosity GRBs. We have therefore repeated the above analysis by selecting

²Note that we are here using the median deviation to characterize the width of the distribution so that, strictly speaking, these are not 1σ errors. Note also that the first point in every distribution has a larger error bar since the corresponding sample is made out of only 4 GRBs with $u \leq u_{th}$ and $u_{th} < 0.095$. We still plot this point for completeness although it is likely statistically meaningless.

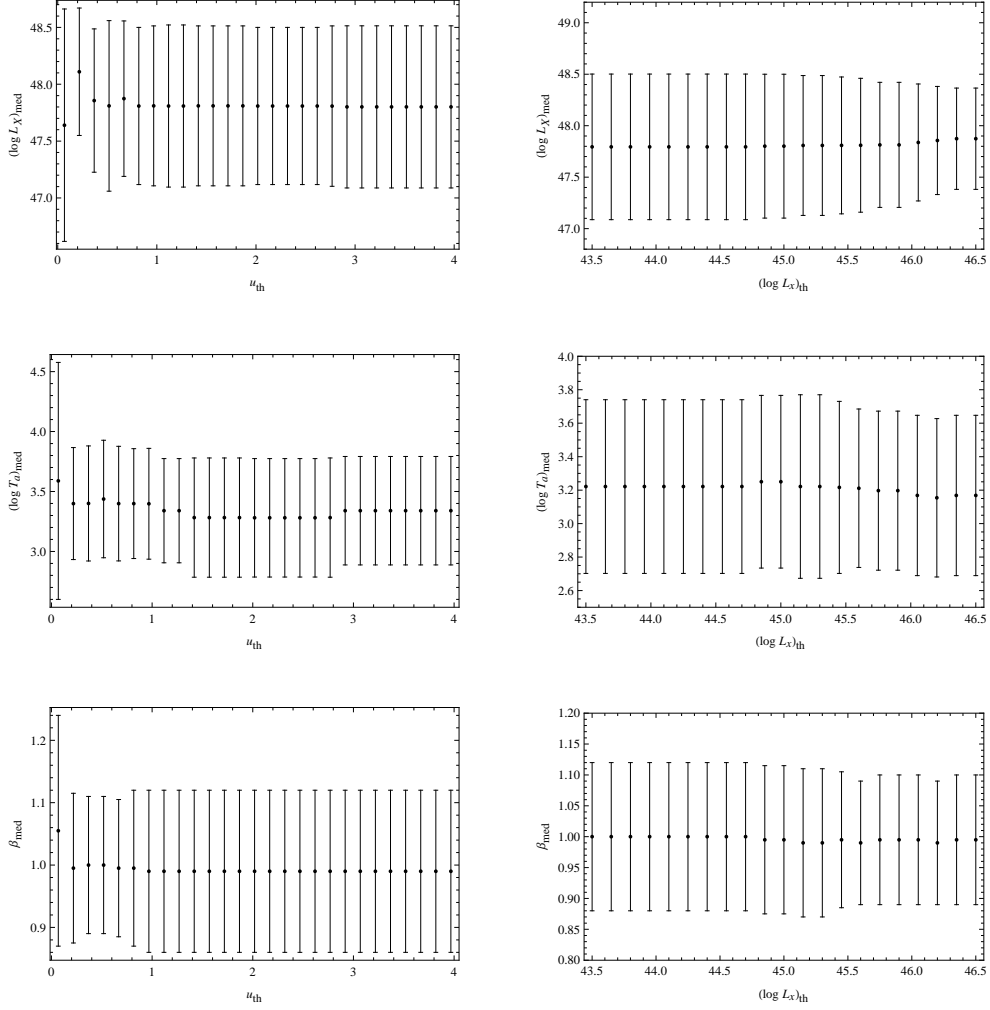


Fig. 5.— Median and median deviation values of $(\log L_X^*, \log T_a^*, \beta_a)$ as function of the threshold values of u (left panels) and $\log L_X^*$ (right panel).

Table 1: Results of the calibration procedure for GRBs divided in three equally populated redshift bins with $(z_{min}, z_{max}) = (0.08, 1.56), (1.71, 3.08), (3.21, 8.26)$ for bins Z1, Z2, Z3.

Id	ρ_{LT}	$(a_{bf}, b_{bf}, (\sigma_{int})_{bf})$	a_{median}	b_{median}	$(\sigma_{int})_{median}$
Z1	-0.69	(-1.20, 51.04, 0.98)	$-1.08^{+0.27}_{-0.30}$	$51.05^{+1.27}_{-0.33}$	$1.01^{+0.20}_{-0.16}$
Z2	-0.83	(-0.90, 50.82, 0.43)	$-0.86^{+0.18}_{-0.16}$	$50.90^{+0.27}_{-0.70}$	$0.45^{+0.09}_{-0.08}$
Z3	-0.63	(-0.61, 50.14, 0.26)	$-0.58^{+0.14}_{-0.15}$	$50.15^{+0.25}_{-0.49}$	$0.26^{+0.07}_{-0.06}$

samples with $\log L_X^* > (\log L_X^*)_{th}$ with $(\log L_X^*)_{th}$ running from 43.50 to 46.50 in steps of 0.15. As shown in the right panels of Fig. 5, such a selection criterion do not bias the sample in $(\log L_X^*, \log T_a^*, \beta_a)$ hence suggesting that the intrinsic scatter of the LT correlation could be reduced by using only moderately bright GRBs. However, since we do not have a physical motivation for applying such a criterion, we have not carried out this analysis.

4. A redshift dependent calibration ?

The redshift range covered by our GRBs sample is quite large with $(z_{min}, z_{max}) = (0.08, 8.26)$ although the distribution is actually quite inhomogenous. Indeed, we have a single GRB at $z = 8.26$ with the second farthest GRBs being at $z = 5.3$. Similarly, the closest GRBs is at $z = 0.08$, but the second one is at $z = 0.12$. The redshift distribution has played, up to now, no role in our analysis since the LT correlation has been fitted to the full GRBs sample thus implicitly assuming that the calibration coefficients (a, b, σ_{int}) are the same over this wide redshift range. It is worth wondering whether this is actually the case. To this end, we have therefore recalibrated the LT correlation dividing the GRBs in three equally populated redshift bins. Note that we use here the fiducial sample ($u < 4$) in order to have a good statistics. If we had chosen, for instance, a set with $u < 0.3$, only 11 GRBs per bin would be present thus leading to large errors preventing any comparison.

The results summarized in Table 1 and shown in Fig. 6 allow us to draw some interesting remarks. Firstly, we note that, although the intrinsic scatter is quite large (mainly because of the use of the fiducial rather than the UP sample), the correlation coefficient ρ_{LT} is quite large in all the redshift bins thus arguing in favour of the existence of LT correlation at any

z . The slopes a for bins Z1 and Z2 are consistent within the 68% CL, while this is not for bin Z3 where the agreement is present only at the 95% CL level. On the contrary, the zeropoint b is consistent among the three bins. Although a trend in the median values of a is present, we therefore can not conclude that the LT correlation becomes shallower for higher redshift GRBs because of the paucity of the sample and the inclusion of large u GRBs. Larger samples with low u values and a more homogenous redshift sampling are needed to solve this issue.

The study of redshift evolution of the LT correlation is particularly interesting in view of its application to cosmology. If the calibration parameters had significantly changed with z , one could have not used the same set of parameters for all the GRBs as, on the contrary, we have usually done. To better clarify this issue, we first remember that the distance modulus

$$\mu = 25 + 5 \log D_L(z) \quad (14)$$

depends on the cosmological parameters as shown by Eq.(7). On the other hand, because of the Eq.(6), the value of μ for a GRB at redshift z may be inferred by the LT correlation as :

$$\begin{aligned} \mu_{obs}(z) &= 25 + \frac{5}{2} \log \left[\frac{L_X^*(T_a)}{4\pi f_a(T_a, T_p, F_a T_a)(1+z)^{(-1+\beta_a)}} \right] \\ &= 25 + \frac{5}{2} \left\{ a \log \left[\frac{T_a}{1+z} \right] + b \right\} \\ &\quad - \frac{5}{2} \log [4\pi f_a(T_a, T_p, F_a T_a)(1+z)^{(-1+\beta_a)}] \end{aligned} \quad (15)$$

with the error estimated as :

$$\sigma_\mu = \frac{5\sigma_{D_L}}{D_L(z) \ln 10} \quad (16)$$

We stress here that the total uncertainty is obtained by adding up the statistical error from the propagation of the errors on the involved quantities and the intrinsic scatter.

We present two tests performed with the aim of understanding if the LT evolves with redshift. We denote with μ_{Zi} and μ_{fid} the values of μ estimated from Eq.(15) using (a, b, σ_{int}) obtained by fitting the Zi and the fiducial samples respectively. Fig.7 presents the plots $\Delta_\mu = \mu_{Zi} - \mu_{fid}$ vs z for the three redshift bins showing that Δ_μ is has a roughly constant behaviour in each redshift bin. Moreover, as shown in Fig.8 (giving instead μ_{Zi}/μ_{fid} as function of z), we can see a flat behaviour too, or at maximum a difference of order $\sim 2\%$, much smaller than the typical error bars and hence fully negligible. We therefore argue a

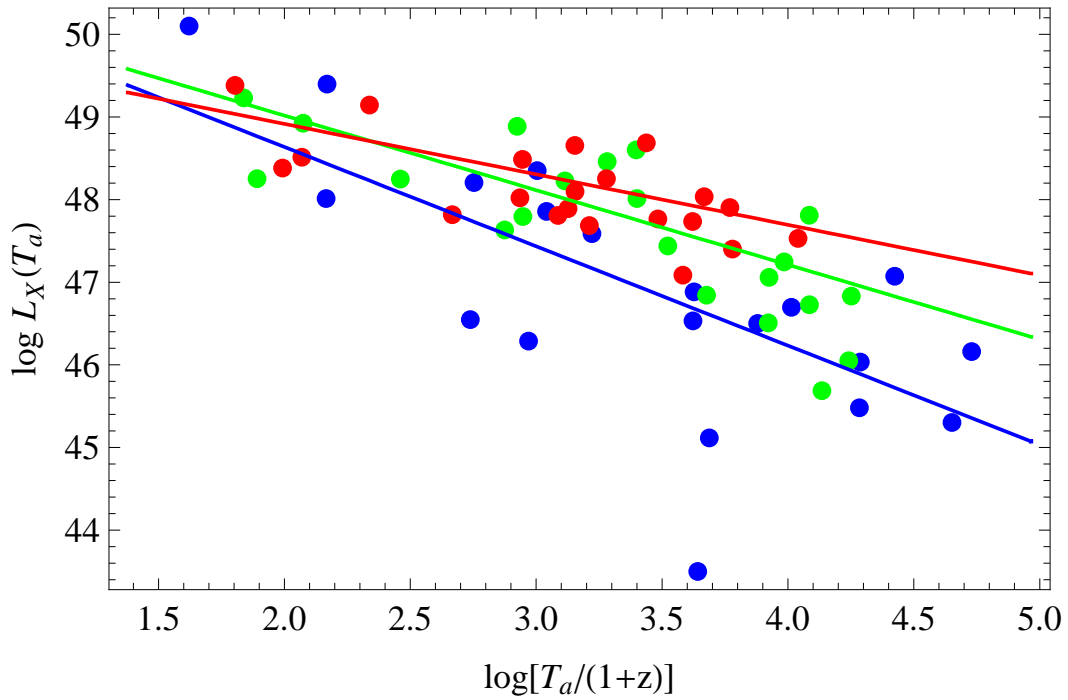


Fig. 6.— $\log L_X^*, \log T_a^*$ correlation divided in the three redshift bins $Z1 = (0.08, 1.56)$, $Z2 = (1.71, 3.08)$ and $Z3 = (3.21, 8.26)$. With the blue points we have represented Z1 sample, with the green ones the Z2 sample and with the red points the Z3 sample. The respective fitted lines are in the same colours.

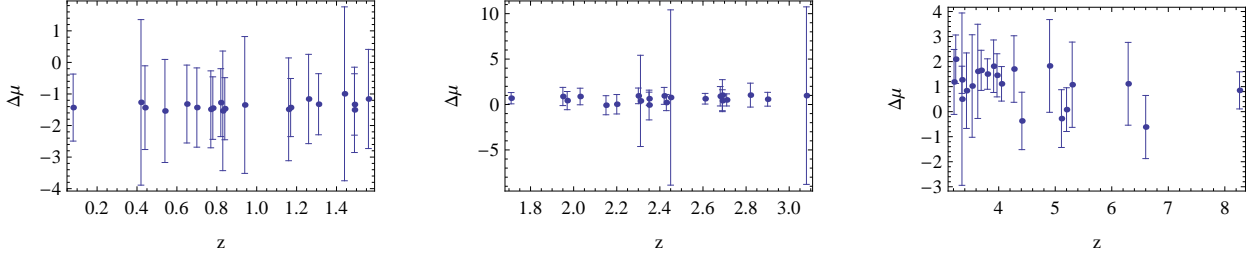


Fig. 7.— $\Delta\mu = \mu_{Zi} - \mu_{fid}$ as function of the redshift z for the three bins Z1 ($0.08 \leq z \leq 1.56$), Z2 ($1.71 \leq z \leq 3.08$), Z3 ($3.21 \leq z \leq 8.26$).

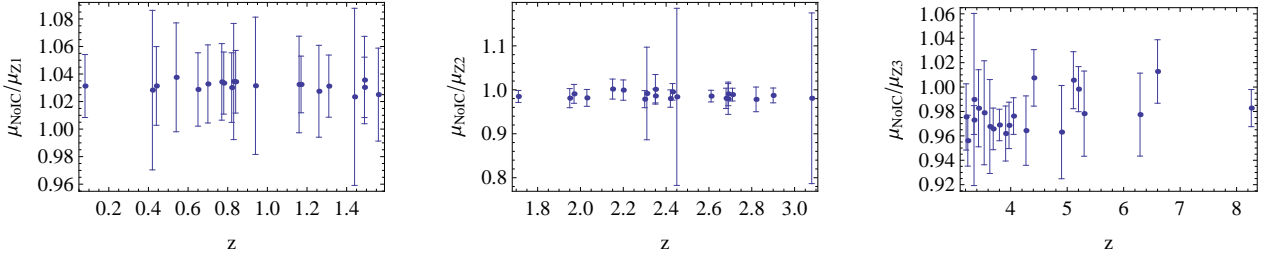


Fig. 8.— Same as Fig. 7 but for the distance modulus ratio μ_{Zi}/μ_{fid} .

(still to be confirmed) redshift dependence of the LT correlation does not preclude its usage as a way to construct a GRBs Hubble diagram (Cardone et al. 2009; Cardone et al. 2009) for cosmological applications.

5. Looking for a redshift estimator

The above analysis has shown that the LT correlation is empirically well motivated and not affected by selection effects due to u selection or to redshift dependent calibration. It is therefore worth investigating its possible applications as redshift estimator. To this aim, let us go back to Eq.(6) and rearrange it in a different way as follows :

$$\begin{aligned}
 \log [L_X^*(T_a)] &= \log (4\pi F_X) + 2 \log D_L(z) - (1 - \beta_a) \log (1 + z) \\
 &= \log (4\pi F_X) + (1 + \beta_a) \log (1 + z) + 2 \log r(z) + 2 \log (c/H_0) \\
 &= a \log \left(\frac{T_a}{1 + z} \right) + b
 \end{aligned} \tag{17}$$

where we have denoted with $r(z)$ the integral in Eq.(7) and, in the last row, we have used the LT correlation with the definition of T_a^* . Solving with respect to z , we get :

$$(1 + \beta_a + a) \log(1 + z) + 2 \log r(z) = a \log T_a + b - \log(4\pi F_X) - 2 \log(c/H_0) \quad (18)$$

For the considered cosmological model, the right hand side of Eq.(18) depends only on measurable quantities so that one can try solving this equation with respect to z to get an estimate of the GRB redshift. There are, however, some preliminary issues that must be considered. First, both the observable quantities (T_a, F_X, β_a) and the LT calibration parameters (a, b) are affected by their own uncertainties. Propagating these errors on the final estimate of z is not analytically possible. Moreover, the uncertainties on (a, b) are not symmetric and the intrinsic scatter σ_{int} (also known with its own asymmetric confidence range) adds to the total uncertainty in a nonlinear way. If we denote by $\mathcal{Z}(\mathbf{p})$ the solution of Eq.(18) for a given set of parameters $\mathbf{p} = \{\log T_a, \log F_X, \beta_a, a, b\}$ and neglect the correlations among the errors, one should estimate the error on z_{est} as:

$$\sigma = \left[\sum \left| \frac{\partial \mathcal{Z}(\mathbf{p})}{\partial p_i} \right|^2 \sigma^2(p_i) \right]^{1/2}$$

where the sum runs over the number of parameters. Actually, such a formula can not be used since, firstly, we do not have an analytical expression for $\mathcal{Z}(\mathbf{p})$ and, secondly, there is actually a non negligible correlation among the parameters (for instance, b is determined from the value of a and σ_{int}). To fully take into account this issue, for each GRB, we first estimate z setting all the observable quantities $(\log T_a, \log F_X, \beta_a)$ to their central values and the calibration parameter (a, b) to their best fit values and solve Eq.(18) to get what we denote as z_{est} .³

We have applied the above test⁴ to the fiducial ($u \leq 4.0$) and the U0095 samples ($u \leq 0.095$) finding out that the LT correlation can still not be used as a redshift estimator,

³Regarding the uncertainty we can only provide a rough estimate repeating the procedure described for a large set of randomly generated values of (a, b) , derived by interpolating the (normalized) histograms outputted from the Markov chains. We then take the histogram of the z_{est} values thus obtained to find out the 68% confidence range (z_{min}, z_{max}) finally defining $\sigma(z_{est}) = [(z_{max} - z_{est}) + (z_{est} - z_{min})]/2$, i.e. we symmetrize the confidence range. It is worth stressing that such an approach implicitly allows us to propagate also the error on σ_{int} since the zeropoint b is determined from the values of (a, σ_{int}) on a case-by-case basis. We don't present in the Fig. 9 the errorbars not to clutter the picture and because for the reasons discussed above they can be only an approximated estimate of the real error measurements.

⁴Remember that, when performing the test, we use the merged chains relative to the fit to the considered sample so that, for instance, the best fit (a, b) values are different in the two cases.

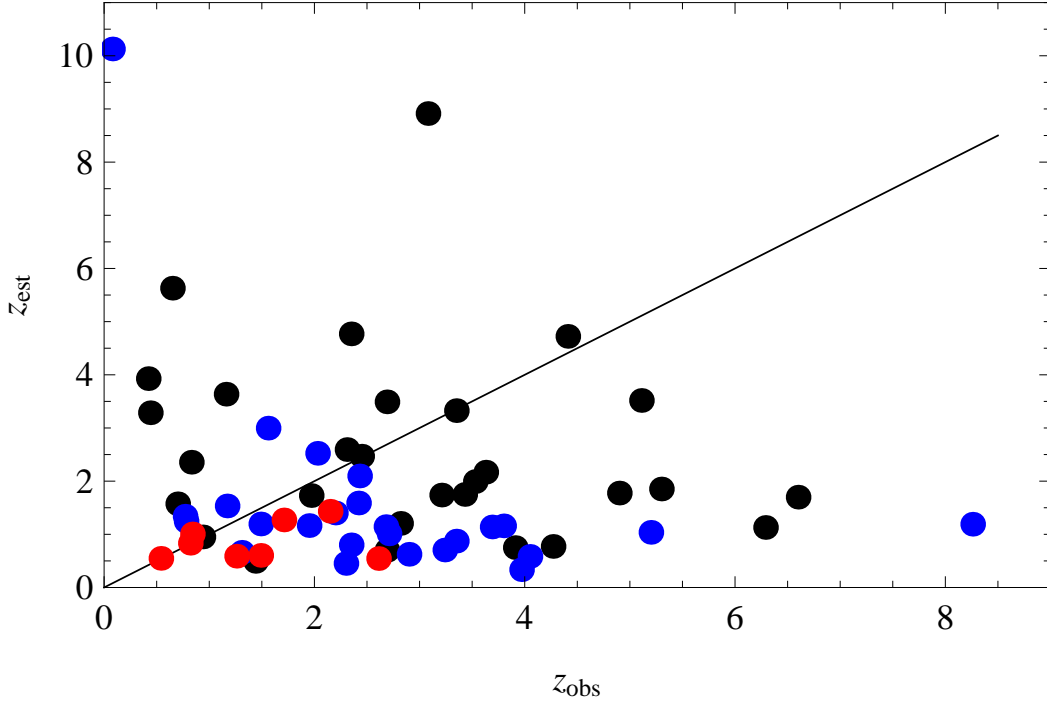


Fig. 9.— Observed vs estimated redshift for the 62 GRBs of the fiducial sample divided in three u bin, i.e, $u \leq 0.095$ (red points), $0.095 \leq u \leq 0.3$ (blue points), $0.3 \leq u \leq 4$ (black points).

as clearly shown in Fig.9. Indeed, defining $\Delta z = z_{obs} - z_{est}$, we get only $\sim 20\%$ (28%) of GRBs in the fiducial (U0095) sample has $|\Delta z / \sigma(z_{est})| \leq 1$. Even if we allow for a very poor precision considering as acceptable estimates those with $|\Delta z / \sigma(z_{est})| \leq 3$, the fraction of successful solutions raises only to a modest $\sim 53\%$ ($\sim 57\%$) for the fiducial (U0095) samples. The qualitative agreement about the bad performance of this estimator for both the fiducial and U0095 samples is a first evidence that the value of u has no impact on the quality of the redshift estimate. This is also shown in Fig.9 where the points closer to the $z_{obs} = z_{est}$ line are not the ones with the smaller u values. Actually, such a result can be easily understood noting that, as yet demonstrated above, the u selection does not bias the samples so that the underlying motivation why this redshift estimator fail applies equally to all GRBs notwithstanding how precise is the measurement of $(\log T_a^*, \log L_X^*)$. Actually, the main motivation of the failure is the intrinsic scatter of the points around the best fit LT correlation. It is quite easy to qualitatively understand this point considering a hypothetical GRB of the U0095 sample with given value of $\log T_a$. Because of the intrinsic scatter of the LT correlation, its estimated intrinsic luminosity $\log L_X$ can be off from the true one up to σ_{int} . Let us denote with L_X^{true} and L_X^{fit} its true and fitted L_X values and let

$L_X(z) = 4\pi D_L(z)^2 F_X(1+z)^{-(1-\beta_a)}$. Our estimate of z is obtained by solving $L_X(z_{est}) = L_X^{fit}$, while it is $L_X(z_{obs}) = L_X^{true}$. Should L_X^{fit} be larger than L_X^{true} , we should increase $D_L(z)$ to compensate for the difference thus overestimating the redshift ($z_{est} > z_{obs}$) with the opposite effect for the $L_X^{fit} < L_X^{true}$ case. This is indeed what happens in our case. Looking at the residuals of the LT correlation, we find that L_X is, on average, underestimated (i.e., $L_X^{fit} < L_X^{true}$) for the higher redshift GRBs so that we expect $z_{est} \leq z_{obs}$ which is indeed what we find looking at the points with $z > 2.5$ in Fig. 9, while the opposite result takes place for very low z GRBs. We can therefore conclude that the LT correlation works satisfactorily well as redshift estimator only for GRBs in the redshift range (0.5, 2.0), while gives severely biased results for smaller and larger z GRBs.

Although these results are quite discouraging, it is nevertheless worth wondering whether the situation can be improved with future data. To this end, we have simulated a U0095 sample generating $(\log T_a^*, \beta_a, z)$ values from a parent distribution closely mimicking the observed one for the fiducial sample⁵. We then set $\log L_X^*$ extracting from a Gaussian distribution centered on the value predicted by the LT correlation and with width equal to the intrinsic scatter. We then use these values to estimate F_X and add noise to all quantities so that the relative errors are the same order as the present day ones. We generate \mathcal{N} GRBs and fit them with the same procedure adopted to find the LT calibration coefficients and use these fake Markov chains as input to the redshift estimate procedure.

It turns out that increasing the sample is not a useful way to improve the performance of the redshift estimator. Indeed, we have found that, with $\mathcal{N} \simeq 50$, the fraction of GRBs with $|\Delta z/\sigma(z_{est})| \leq 1$ first increases to $\sim 34\%$ and then decreases to $\sim 20\%$ for $\mathcal{N} \simeq 200$, while $\langle \Delta z/z_{obs} \rangle \simeq -17\%$ for both $\mathcal{N} \simeq 50$ and $\mathcal{N} \simeq 200$, a significant improvement with respect to the value quoted above, but still not fully satisfactory considering that $rms(\Delta z/z_{obs}) \simeq 75\%$. It is somewhat counterintuitive that increasing the sample does not improve the quality of the redshift estimator. Actually, such a result could be anticipated noting that a larger sample leads to stronger constraints on the (a, b, σ_{int}) values, but do not change the intrinsic scatter which is the main source of possible mismatches between the true and fitted GRB luminosity. Motivated by this consideration, we therefore perform a second test artificially lowering the intrinsic scatter σ_{int} , but setting the best fit (a, b) parameters to those derived from the fit to the U0095 sample. Indeed, for $\mathcal{N} = 50$ and $\sigma_{int} = 0.20$, we get $\langle \Delta z/z_{obs} \rangle \simeq -3\%$ with $rms(\Delta z/z_{obs}) \simeq 28\%$ and 46% (87%) of GRBs with $|\Delta z/\sigma(z_{est})| \leq 1$ (≤ 3). Again increasing the sample to $\mathcal{N} \simeq 200$ has not a significant impact, while a stronger impact

⁵Note that this choice is motivated by the poor statistics of the present U0095 sample. We have, however, checked that the U0095 GRBs cover the same region in the $(\log T_a, \beta_a, z)$ parameter space as the fiducial ones.

is obtained setting $\sigma_{int} = 0.10$ giving $\langle \Delta z / z_{obs} \rangle \simeq -0.6\%$ with $rms(\Delta z / z_{obs}) \simeq 16\%$ and $f(|\Delta z / z_{obs}| \leq 1) \simeq 66\%$. These results convincingly show that the LT correlation could be used as a redshift estimator only if a subsample of the canonical GRBs could be identified in such a way to reduce the intrinsic scatter to $\sigma_{int} = 0.10 - 0.20$. It is worth wondering whether assembling such a sample is indeed possible. Actually, a detailed answer can not be given since our U0095 sample is too small to find out some indicator that can help to find out GRBs less scattering from the best fit LT correlation. A visual inspection of the fit residuals makes us roughly argue that σ_{int} could be reduced using only 5 out of the 8 U0095 GRBs which represent $\sim 8\%$ of the fiducial GRBs sample. If we assume this fraction as a constant, one should assemble a sample of ~ 600 GRBs with measured values of $(\log T_a^*, \log L_X^*, \beta_a, z)$ to get ~ 50 GRBs to calibrate the LT correlation with $\sigma_{int} \sim 0.20$. While this is for sure an ambitious task, it is worth noting that it is still possible that a smaller sample is enough to find out the observable properties of these GRBs thus allowing an easier search and reducing the number of GRBs to be followed up for the z estimate.

6. Summary

The analysis presented here have shown that the LT correlation, for both the fiducial and UE samples, is not affected by selection effects induced by the u threshold selection or by the implicit assumption of redshift independence of the calibration parameters. In particular, the selection on u does not bias the distribution of the $(\log L_X^*, \log T_a^*, \beta_a)$ quantities thus showing that the canonical GRBs ($u < 0.095$) in the U0095 sample are indeed distributed preferentially in the upper part of the LT plane. This is a further evidence that the afterglow light curves which are smooth and well fitted by the W07 model indeed define a physically homogenous class with the remarkable feature of obeying a well defined empirical correlation. Furthermore, the analysis presented also pinpoints the existence of a well defined correlation of the X-ray spectral index β_a with the rest frame break time T_a^* which deserves further analysis.

As an important result, we have also shown that, although a shallowing of the LT correlation for higher z GRBs can still not be totally excluded, its impact on the distance modulus estimate is negligible thus validating the usage of this correlation as a new independent cosmological tool (Cardone et al. 2009). As a first application, Cardone et al. (2010) have indeed derived the Hubble diagram using the LT correlation only and shown that, when combined with other distance probes (such as Type Ia Supernovae and Baryon Acoustic Oscillations), GRBs are a valuable tool to constrain the cosmological parameters. To this end, Cardone et al. (2010) have used the full fiducial sample to increase the statistics, but at the

price of including GRBs with large errors on the distance modulus. It is worth wondering how large a GRB sample should be to improve the constraints on the cosmological parameters. Such a problem has yet been addressed by some of us (Cardone et al. 2009) using the Fisher matrix analysis and the first version of the LT correlation. There, we have shown that combining a sample of 200 GRBs with a SNAP-like SNeIa sample allows to determine the matter density parameter Ω_M and the dark energy equation of state parameters (w_0, w_a) within 0.019, 0.036, 0.020, respectively. In particular, GRBs are of extremely importance to constrain Ω_M giving an improvement in precision of a factor 4 with respect to the case when SNeIa only are used. Although these results refer to the first version of the LT correlation and thus refer to a sample with no selection on u , they qualitatively hold also in our case since the basic inputs to the Fisher matrix analysis are essentially the same. Actually, having made no cut on u , the quoted results are likely to be quite conservative since the u selection allows to reduce the scatter and hence the error on the distance modulus thus increasing the efficiency of GRBs with respect to the case considered in Cardone et al. (2009).

We have, finally, investigated the possibility to use the LT correlation as a redshift estimator obtaining actually discouraging results for both the fiducial and U0095 samples. Having qualitatively discovered the reason of this failure, we have shown that reducing the intrinsic scatter of the LT correlation could help to calibrate an improved LT correlation that could work as a tool to estimate the GRB redshift from the analysis of its X-ray afterglow lightcurve. However, we are not sure if it is possible to obtain a reduced intrinsic scatter of the correlation with the real data measurements related to the U0095 sample.

Acknowledgments

This work made use of data supplied by the UK Swift Science Data Centre at the University of Leicester. MGD and MO are grateful for the support from Polish MNiSW through the grant N N203 380336. MGD is also grateful for the support from Angelo Della Riccia Foundation.

REFERENCES

- L. Amati, F. Frontera & C. Guidorzi A&A, 508, 173.
- Arnaud, K. 1996, in *Astronomical data analysis software and systems*, Jacoby G., Barnes, J. eds., ASP Conf. Series, Vol. 101, p17
- Band, D., Matteson, J., Ford, L. et al., ApJ, 413, 281 (1993)

- Butler, N. R., Bloom, J. S., Poznanski, D. arXiv:0910.3341 (2009)
- Cabrera J. I., Firmani, C., Ghisellini, et al. Mon. Not. R. Astron. Soc. 382, 342 (2007)
- Cardone, V.F, Dainotti, M.G., Capozziello, S. & Willingale, R. Mon. Not. R. Astron. Soc. 400, 775 (2009)
- Cardone, V.F, Capozziello, S. & Dainotti, M.G. Mon. Not. R. Astron. Soc. 400, 775 (2010)
- Bloom, J.S., Frail, D.A., Sari, R. Astron. J. 121, 2879-2888 (2001)
- D' Agostini, G. 2004, arXiv : physics/0403086
- D' Agostini, G. 2005, arXiv : physics/051182
- Dainotti, M.G., Cardone, V.F., Capozziello, S. Mon. Not. R. Astron. Soc. 391, L79-L83 (2008)
- Dainotti, M.G., Willingale, R., Cardone, V.F, Capozziello, S. & M. Ostrowski ApJL, 722, L 215 2010.
- Freedman, W.L., Madore, B.F., Gibson, B.K., Ferrarese, L., Kelson, D.D., Sakai, S., Mould, J.R.; Kennicutt, R.C. et al., ApJ, 553, 47, 2001
- Gelman, A. & Rubin, D.B. 1992, Statistical Science, 7, 457.
- Ghisellini G., Nava L., Ghirlanda G., Firmani C., et al. 2008, A & A, 496, 3, 2009.
- Ghirlanda G., Ghisellini G. & Firmani C., 2006, New Journal of Physics, 8, 123.
- E.J. Komatsu, et al., preprint arXiv:1001.4538, 2010
- Kowalski, M., Rubin, D., Aldering, G., Agostinho, R.J, Amadon, A. et al. 2008, arXiv:0804.4142
- Norris, J.P, & Bonnell, J.T. 2006, ApJ, 643, 266.
- Nousek, J.,A. et al. 2006, ApJ 642, 389.
- O' Brien, P.T., Willingale, R., Osborne, J. et al. 2006, ApJ, 647, 1213.
- Piro, L. 2001, in Gamma-ray Bursts in the Afterglow Era: proceedings, Costa, E., Frontera, F. & Hjorth, J. eds., Springer,Verlag, pp. 97.
- Riechart, D.E., Lamb, D.Q., Fenimore, E.E., Ramirez - Ruiz, E., Cline, T.L. 2001, ApJ, 552, 57 2007.

Spearman, C. The American Journal of Psychology, 15, 72 (1904)

Schaefer, B.E. 2003, ApJ, 583, L67

Shahmoradi, A. & Nemiroff R. J. arXiv0904.1464S (2009)

Willingale, R.W. et al., ApJ. 662, 1093-110 2007

Yamazaki,R. (2009), Apj, 690, L118.

Yu, B., Qi, S., Lu, T. Astrophys. J. Letters 705 L15-L19 (2009)

